ELSEVIER

Journal of Alloys and Compounds 1 (2002) 000–000

Journal of ALLOYS AND COMPOUNDS

www.elsevier.com/locate/jallcom

Atomistic simulation of the lattice constants and lattice vibrations in RT_4Al_8 (R=Nd, Sm; T=Cr, Mn, Cu, Fe)

Yan-mei Kang[a,*], Nan-xian Chen[a,b], Jiang Shen[b]

[a]*Department of Physics, Tsinghua University, Beijing 100084, China*

[b]*Institute of Applied Physics, University of Science and Technology Beijing, Beijing 100083, China*

Received 14 August 2002; accepted 3 October 2002

Abstract

The lattice constants of the rare earth intermetallic compounds RT_4Al_8 (R=Nd, Sm; T=Cr, Mn, Cu, Fe) with $ThMn_{12}$-type structure were evaluated. This calculation was based on the interatomic potentials related to the rare earth and transition metals, which were obtained by a lattice inversion method. The results are in agreement with experiments. The total and partial phonon densities of states for these materials are also presented. The analysis for the inverted potentials explains qualitatively the contributions of different atoms to the vibrational modes.

Keywords: Rare earth compounds; Transition metal compounds; Lattice dynamics; Computer simulations

1. Introduction

The aluminium rare earth compounds RT_xAl_{12-x} (R= rare earth and T=transition metal) crystallize in the relatively simple $ThMn_{12}$-type structure, which belongs to the $I4/mmm$ space group. There are 26 atoms per unit cell. For RT_4Al_8, neutron diffraction has shown that T atoms occupy almost exclusively the 8*f* sites, Al atoms the 8*j* and 8*i* positions and R atoms the 2*a* sites [1,2]. With increasing T content the 8*j* and 8*i* positions are also occupied by T with the Al atoms. These compounds exhibit interesting magnetic properties, which have received considerable attention [1–5].

The atomistic simulation is an effective approach to achieve a better understanding of the structures and properties of the materials, of which the proper interatomic potentials are highly important. Many empirical interatomic pair potentials such as the Buckingham potential, the Lennard–Jones potential, the Morse potential and the Born–Mayer potential [6] have been widely used in the atomistic simulation of various kinds of materials [7,8]. However, due to the inherent drawback of the pair potentials [9] many-body potential models have been constructed in past decades. For example, the Finnis–Sinclair model [10,11] and glue model [9] are used extensively in the transition metals and alloys, of which the embedded atom model (EAM) is more widely used [12–14]. The empirical many-body potential model includes adjustable parameters which are determined by fitting some experimental data of the involved systems. The forms of the embedding function, pair potential function and electron density function used in the EAM model are related to the concrete structures of metals. However, sometimes it is hard to obtain some reliable experimental data such as the elastic modulus of the bristle materials and the single vacancy formulation energy that may be distinct with different experimental methods. So, the applications of empirical many-body potential models are limited in rare earth intermetallic compounds with complex structures. Recently, the semi-empirical [15] and EAM [16] interatomic potentials of rare earth metals and the binary alloys of Mg, Ni and rare earth metals have been developed [17,18]. These potential parameters were also adjusted to reproduce some experimental data.

In this work, the lattice inversion technique [19–22] was applied to obtain systematically a series of interatomic potentials related to RT_4Al_8 (R=Nd, Sm; T=Cr, Mn, Cu, Fe) from the first-principle cohesive energy calculations. Based on these calculated potentials, the cohesive energies while T atoms occupy the different sites were calculated. The sites corresponding to the lowest energies are exactly

*Corresponding author. Tel./fax: +86-10-6277-2783.
E-mail address: kangyanmei@yahoo.com.cn (Y.-M. Kang).

0925-8388/02/$ – see front matter
PII: S0925-8388(02)01134-9

the preferential occupations of the ternary elements. The evaluated lattice parameters of these materials are in agreement with the experimental data. These calculations explore the complex structures of these kinds of materials using the interatomic potentials. In addition, several simple mechanical properties were investigated. Particularly, some lattice vibrational properties for these rare earth compounds were evaluated, from which the Debye temperatures were obtained.

2. Calculation method

The idea of the inversion technique for generating the parameter-free pair potential was first suggested by Carlsson et al. [23]. This technique was based on two assumptions, that the cohesive energy can be written as a sum of pair interaction energies and the electronic structure calculations of the cohesive energy are a function of volume. The expression for their pair potentials includes infinite summations, each of them contains infinite terms. This made it inconvenient for analysis. In the mid-1990s, based on the same assumptions, Chen et al. developed a concise inversion method based on the modified Möbius inversion transform in number theory to avoid the above shortcomings [19–22]. The calculation of the cohesive energy is based on the virtual simple structure and deduced from the total energy of the sublattice. The interatomic potentials between the distinct atoms can also be obtained by the procedure. So it is convenient for analysis since the inversion coefficient of materials with identical structure is concise and uniform. This method has been applied successfully to study the field-ion microscopy image of Fe_3Al analysis [22], the site preference of ternary additions in Fe_3Al [24], the lattice dynamics of zinc-blend-type binary compounds [25], the mechanical and thermal properties of some metal hydride [26] and so on. An introduction to this lattice inversion method was given in our previous work [27–29].

In this work, the total energy ab initio calculations (ESOCS 4.0 program provided by Materials Simulation Incorporation) were performed on the basis of an augmented spherical-wave method [30,31] within the local density functional theory. The cohesive energy is obtained from

$$E(x) = E_{\text{tot}}(x) - E_{\text{tot}}(\infty).$$

A series of functions $E(x)$ are calculated with various lattice constants at equal intervals of 0.1 Å. In each case, for generating the total energy, more than 80 k-points in an irreducible Brillouin zone are taken into account in a self-consistent calculation. The data are then fitted on the basis of Rose functions. The obtained pair potential can be generally described by Morse function:

$$\Phi(R) = D_0\{\exp[-2\alpha(R - R_0)] - 2\exp[-\alpha(R - R_0)]\}$$

Table 1
Part of potential parameters acquired from the inversion method

Potential types	D_0 (eV)	α	R_0 (Å)
Nd–Al	0.4865	1.5030	3.4146
Nd–Cr	0.5278	1.3355	3.2885
Nd–Mn	0.5980	1.3638	3.2907
Nd–Cu	0.4459	1.8716	3.2934
Nd–Fe	0.6036	1.6458	3.1889
Sm–Al	0.4302	1.5632	3.3634
Sm–Cr	0.5194	1.2921	3.2568
Sm–Mn	0.6157	1.4427	3.2152
Sm–Cu	0.4482	1.7985	3.2674
Sm–Fe	0.5888	1.4885	3.1394

where R is the distance between two atoms, D_0, α, R_0 are the parameters. Some of the potential parameters are listed in Table 1. To give an intuitive impression, the calculated interatomic potentials Φ_{R-R}, Φ_{Al-Al}, Φ_{R-Al}, Φ_{R-T}, Φ_{Al-T}, Φ_{T-T} (R = Nd, Sm; T = Cr, Mn, Cu, Fe) are shown in Fig. 1.

3. Cohesive energies and lattice constants of RT_4Al_8 (R = Nd, Sm; T = Cr, Mn, Cu, Fe)

In the calculation, the initial lattice constants of the metastable $NdAl_{12}$ and $SmAl_{12}$ were randomly chosen in a certain range. Under the influence of the interatomic potentials, energy minimization was performed using the conjugate gradient method. The results show that the final structures can stabilize to tetragonal with the space group $I4/mmm$ within a tolerance 0.01 Å. The tolerance range indicates the atomic derivation distance, which can be viewed as the error in the process of determining the space group of the compound. The crystal constants are $a = 9.539$ Å, $c = 5.447$ Å (Table 2) for $NdAl_{12}$. For $SmAl_{12}$ the lattice constants are $a = 9.549$ Å, $c = 5.430$ Å, which were obtained by a similar procedure as in $NdAl_{12}$. The presence of a certain amount of randomness of the initial structure and the stability of the final structure illustrate that the RAl_{12} has a topological invariability with respect to the stably existing RT_4Al_8 (T = Cr, Cu, Mn, Fe). The RAl_{12} compounds can be considered as the intrinsic structure of the RT_4Al_8. As sample systems we chose $(NdAl_{12})_{16}$ and $(SmAl_{12})_{16}$ as crystal cells with periodic boundaries and introduced relaxation governed by the interaction of pair potentials, using the conjugate gradient method with a cut-off radius of 14 Å. The energy values in Tables 3 and 4 are the results when four T atoms distribute over the 8i, 8j and 8f sites, respectively. It shows obviously that the system is in higher energy states when T atoms occupy the 8i or 8j sites. The cohesive energy is lowest when T atoms are substituted for Al atoms at the 8f sites. It corresponds to the preferential site occupation of T in the experiments [1,32,33].

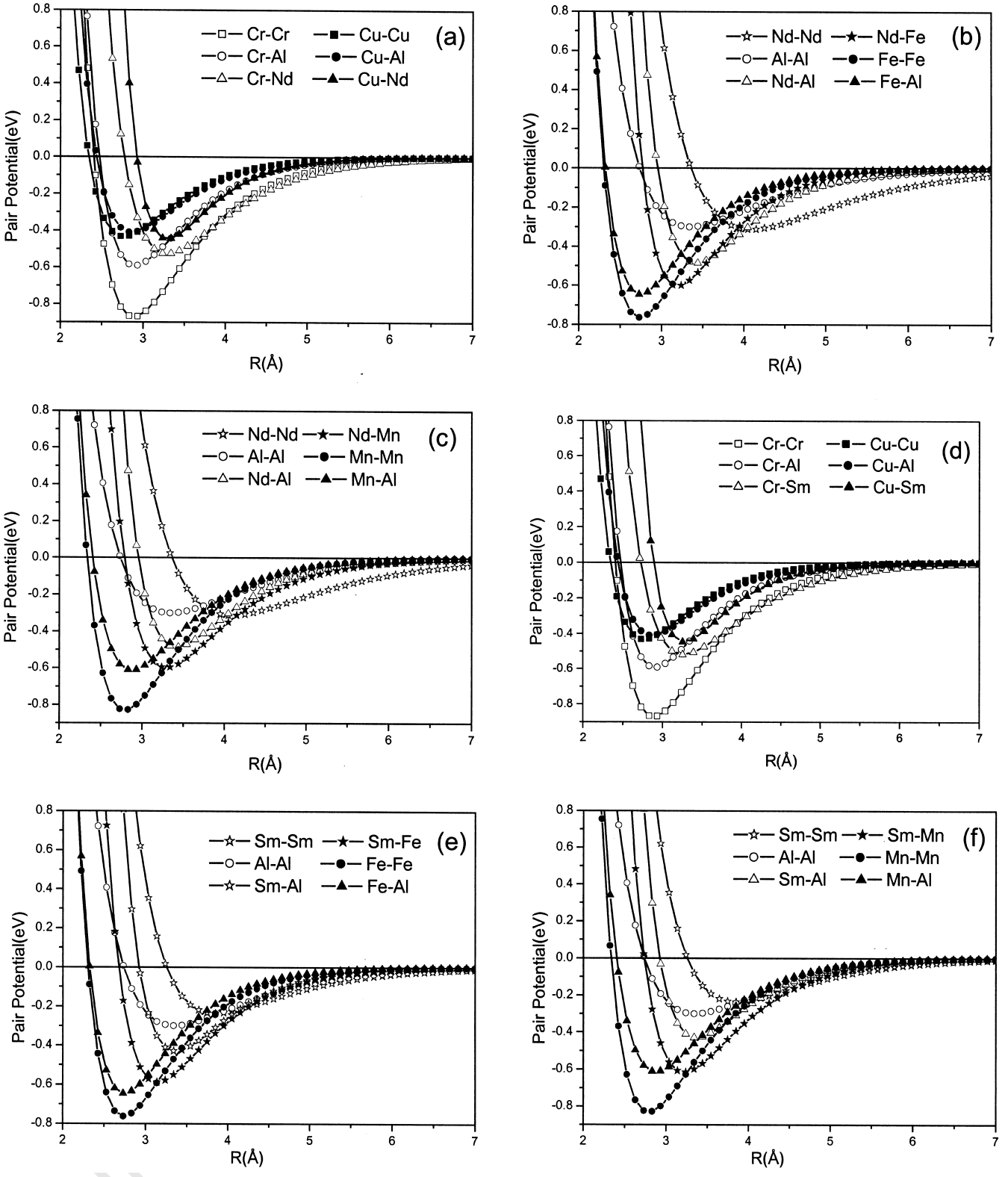

Fig. 1. Potentials of R–T–Al (R = Nd, Sm; T = Cr, Mn, Cu, Fe).

According to the results of the site preference, using the conjugate gradient method the lattice constants of RT_4Al_8 (R = Nd, Sm; T = Cr, Mn, Cu, Fe) were calculated when T atoms exclusively occupy the 8*f* sites. The results are listed in Table 5. These crystal constants can also be obtained by a similar procedure to that of $NdAl_{12}$ as shown in Table 2. For the two compounds composed of identical ternary atoms and distinct rare earth atoms, the difference of their

Table 2
Lattice constants of $NdAl_{12}$

Initial states			Final states		
a, *b*, *c* (Å)	*α*, *β*, *γ* (deg)	Space group	*a*, *b*, *c* (Å)	*α*, *β*, *γ* (deg)	Space group
5, 5, 3	90, 90, 90	$I4/mmm$	9.539, 9.539, 5.447	90, 90, 90	$I4/mmm$
18, 18, 10	90, 90, 90	$I4/mmm$	9.539, 9.539, 5.447	90, 90, 90	$I4/mmm$
9, 9, 5	80, 70, 120	$P\bar{1}$	9.539, 9.539, 5.447	90, 90, 90	$I4/mmm$
5, 5, 3	80, 80, 80	$C2/m$	9.539, 9.539, 5.447	90, 90, 90	$I4/mmm$
15, 15, 7.5	100, 90, 80	$P\bar{1}$	9.539, 9.539, 5.447	90, 90, 90	$I4/mmm$
5, 5, 6	100, 80, 70	$C2/m$	9.539, 9.539, 5.447	90, 90, 90	$I4/mmm$
15, 10, 9	70, 80, 100	$P\bar{1}$	9.539, 9.539, 5.447	90, 90, 90	$I4/mmm$
5, 11, 7	80, 70, 65	$P\bar{1}$	9.539, 9.539, 5.447	90, 90, 90	$I4/mmm$
15, 7, 4	80, 80, 80	$P\bar{1}$	9.539, 9.539, 5.447	90, 90, 90	$I4/mmm$
5, 6, 9	80, 80, 65	$P\bar{1}$	9.539, 9.539, 5.447	90, 90, 90	$I4/mmm$
13, 14, 8	80, 95, 110	$P\bar{1}$	9.539, 9.539, 5.447	90, 90, 90	$I4/mmm$
5, 5, 2.5	60, 60, 60	$C2/m$	9.586, 9.586, 5.415	90, 90, 90	$I4\ mm$

Table 3
Calculated cohesive energies of NdT_4Al_8 (T=Cr, Cu, Mn, Fe) and $NdAl_{12}$

		$NdCr_4Al_8$	$NdCu_4Al_8$	$NdMn_4Al_8$	$NdFe_4Al_8$	$NdAl_{12}$
Cohesive energy	8*i* site	−4.240	−3.157	−4.387	−4.138	
(eV/atom)	8*j* site	−4.181	−3.279	−4.383	−4.229	−3.223
	8*f* site	−4.286	−3.440	−4.520	−4.407	

Table 4
Calculated cohesive energies of SmT_4Al_8 (T=Cr, Cu, Mn, Fe) and $SmAl_{12}$

		$SmCr_4Al_8$	$SmCu_4Al_8$	$SmMn_4Al_8$	$SmFe_4Al_8$	$SmAl_{12}$
Cohesive energy	8*i* site	−4.131	−3.044	−4.257	−4.035	
(eV/atom)	8*j* site	−4.076	−3.182	−4.282	−4.126	−3.083
	8*f* site	−4.200	−3.363	−4.422	−4.333	

lattice constants is small, which is in agreement with experimental data. In addition, the calculated lattice constants, *a* and *c*, are a little larger than the experimental data [33–37] except for *a* of $SmFe_4Al_8$. The average deviation is 2.256% with the largest 4.576% from the experiment. The error can be explained by the fact that for RT_4Al_8 the

Table 5
Comparison between the calculated and experimental lattice parameters *a* and *c* for $NdAl_{12}$, NdT_4Al_8 and $SmAl_{12}$, SmT_4Al_8 (T=Cr, Cu, Mn, Fe)

Materials	*a*			*c*		
	Cal. (Å)	Exp. (Å)	Err. (%)	Cal. (Å)	Exp. (Å)	Err. (%)
$NdAl_{12}$	9.539	–	–	5.447	–	–
$NdCr_4Al_8$	9.182	9.000[a]	2.022	5.371	5.136[a]	4.576
$NdCu_4Al_8$	9.169	8.789[b]	4.324	5.253	5.143[b]	2.139
$NdMn_4Al_8$	9.061	8.937[c]	1.387	5.226	5.136[c]	1.752
		8.925[b]	1.524		5.133[b]	1.182
$NdFe_4Al_8$	8.875	8.813[d]	0.704	5.211	5.058[d]	3.025
		8.804[e]	0.806		5.054[e]	3.106
$SmAl_{12}$	9.549	–	–	5.430	–	–
$SmCr_4Al_8$	9.177	8.973[a]	2.273	5.355	5.136[a]	4.264
$SmCu_4Al_8$	9.159	8.797[b]	4.115	5.230	5.143[b]	1.692
$SmMn_4Al_8$	9.031	8.902[b]	1.449	5.213	5.120[b]	1.816
$SmFe_4Al_8$	8.863	8.773[d]	1.026	5.188	5.051[d]	2.712
		8.770[e]	1.060		5.053[e]	2.672

[a] Ref. [35].
[b] Ref. [36].
[c] Ref. [34].
[d] Ref. [37].
[e] Ref. [33].

Table 6
Elastic constants C_{ij} and bulk moduli of $Nd(Al,T)_{12}$ and $Sm(Al,T)_{12}$ (T=Cr, Cu, Mn, Fe)

Materials	Elastic constants C_{ij} (GPa)						Bulk modulus
	C_{11}	C_{12}	C_{13}	C_{33}	C_{44}	C_{66}	(GPa)
$NdCr_4Al_8$	317.21	44.26	89.30	290.66	87.07	41.07	152.18
$NdCu_4Al_8$	279.95	44.98	72.90	245.21	67.19	44.18	131.83
$NdMn_4Al_8$	322.02	47.13	87.30	316.71	81.05	46.55	155.61
$NdFe_4Al_8$	370.11	55.84	95.30	344.86	89.37	55.23	175.27
$SmCr_4Al_8$	310.30	46.47	86.93	280.92	85.99	41.98	149.08
$SmCu_4Al_8$	274.33	45.64	71.12	237.68	66.99	45.51	129.07
$SmMn_4Al_8$	319.40	47.82	85.87	310.23	81.73	46.98	153.95
$SmFe_4Al_8$	362.37	54.62	92.15	337.73	89.08	54.92	171.10

8*f* sites are the majority sites for T atoms but a small amount of sites are also for Al atoms [33,34]. In addition, the stoichiometry of RT_4Al_8 exhibits compositions different from the 1:4:8 ratio even in single crystals of these materials [38,39]. In the calculation, it was assumed that RT_4Al_8 has a relatively perfect periodic crystal structure and four T atoms entirely distribute over the 8*f* sites. These assumptions may result in a deviation of the calculations from the experimental data.

4. Elastic constants and bulk moduli for RT_4Al_8 (R=Nd, Sm; T=Cr, Mn, Cu, Fe)

Generally the mechanical properties of the rare earth intermetallic compounds could hardly be measured experimentally. It needs a huge computer capacity to calculate them by an ab initio method due to their complex structures. In this work the elastic constants and the bulk moduli of RT_4Al_8 (R=Nd, Sm; T=Cr, Mn, Cu, Fe) were

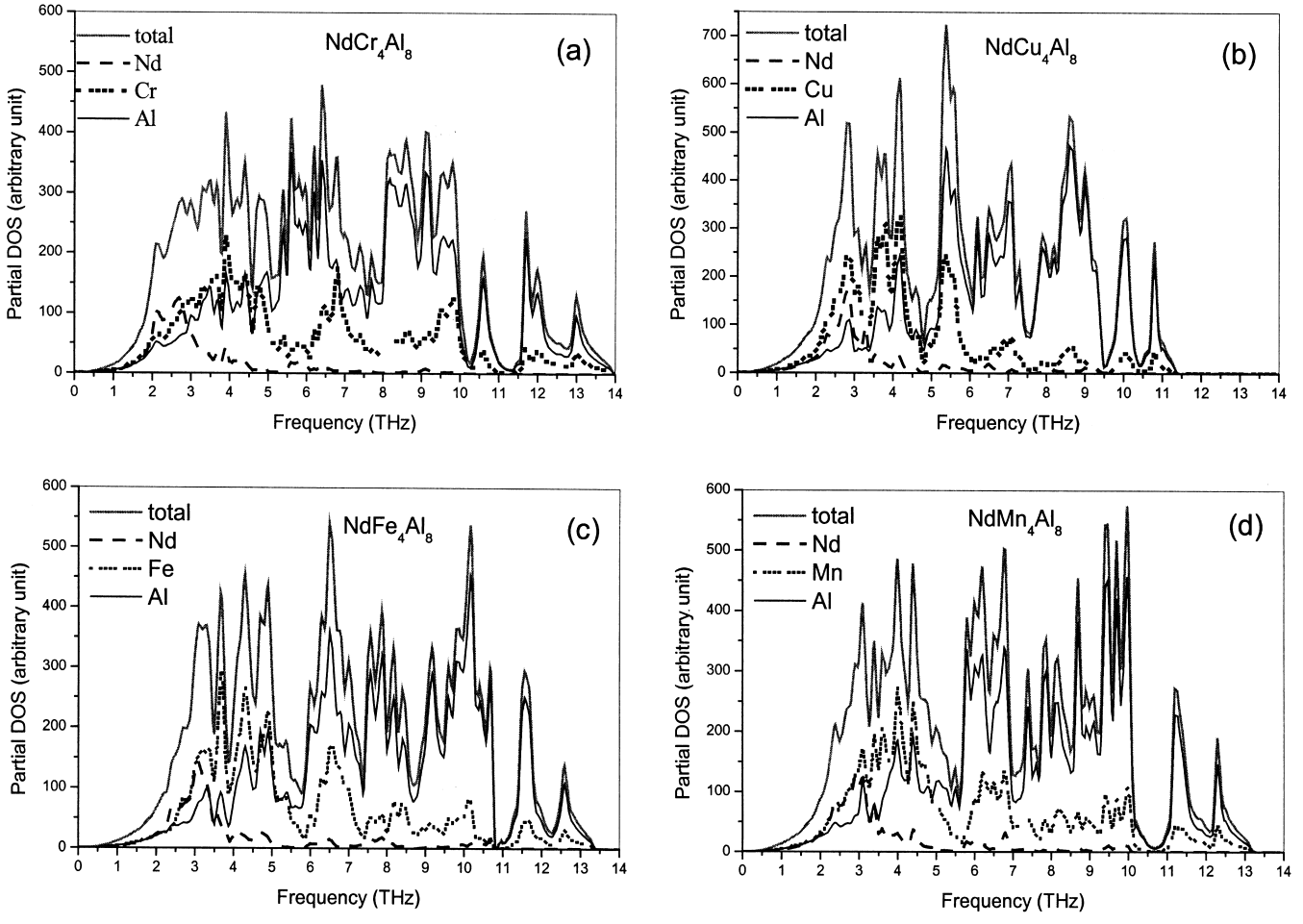

Fig. 2. Phonon densities of states of $NdCr_4Al_8$ (a), $NdCu_4Al_8$ (b), $NdFe_4Al_8$ (c) and $NdMn_4Al_8$ (d).

evaluated by the inverted pair potentials. The results are listed in Table 6.

As Table 6 shows, $SmFe_4Al_8$ and $NdFe_4Al_8$ have the largest values for the bulk moduli and for each component of the elastic constants while $SmCu_4Al_8$ and $NdCu_4Al_8$ have the lowest values for the bulk moduli and for almost all elastic constant components. The RT_4Al_8 compounds of variable T component but fixed rare earth component possess similar mechanical properties. It demonstrates that the ternary element T plays a role regarding the mechanical properties of these materials.

5. Phonon densities of states for RT_4Al_8 (R=Nd, Sm; T=Cr, Mn, Cu, Fe)

For the rare earth compounds, due to the low symmetry of the complex structure, it is difficult to calculate and measure their phonon spectra. Recently, we have studied the lattice dynamics of $ScCu_4Al_8$ [40] and $Ce_xSc_{1-x}Fe_4Al_8$ [28] using the inverted interatomic potentials. In this subsection, based on the lattice theory, the total phonon densities of states as well as the partial DOS of different elements for RT_4Al_8 (R=Nd, Sm; T=Cr, Mn, Cu, Fe) were evaluated in a crystal cell including 26 atoms. The results of NdT_4Al_8 compounds are shown in Fig. 2. It can be seen that the highest frequencies of the phonon density states are 13.97, 13.39, 13.22 and 11.37 THz for T=Cr, Fe, Mn, Cu, respectively. For every spectrum, it can be divided into two parts at about 10.2, 10.8, 10.7 and 9.5 THz, respectively, where the phonon density is almost zero. The second part is called high frequency localized modes. In the spectra of $NdCr_4Al_8$, the first part can be roughly separated into three subsections: 0–5, 5–8 and 8–10 THz. The Nd atoms only contribute to the lower frequency vibrations because of their heavier mass, while the Cr and Al atoms contribute to the higher frequency vibrations and the high frequency localized modes. The contribution of Al is much larger than that of Cr and the ratio between them is about 3:1.

One can analyze qualitatively the vibrational modes from interaction potentials (Fig. 1a) and the nearest neighbor distances between the atoms. Firstly, there are four Al atoms at the 8*i* site, eight Al atoms at the 8*j* site and eight Cr atoms at the 8*f* sites around Nd. The distances between Nd and these atoms are 3.20, 3.32 and 3.51 Å, respectively, for the relaxed structure of $NdCr_4Al_8$. As shown in Fig. 1a, Nd reacts strongly with Al and Cr at these distances. The mass of Nd is much larger than that of Al and Cr, so it is assumed motionless relative to Al and Cr atoms. Then some of the Al atoms and Cr atoms are restricted in the 'potential well' $\Phi_{Nd-Al}(r)$ and $\Phi_{Nd-Cr}(r)$. This might be the reason for the appearance of the localized modes of Al atoms and Cr atoms, which correspond to higher transverse frequencies. Though the interaction between Nd and Cr is intense at their nearest distance, the Cr atoms cannot be excited by more modes with higher frequency than the Al atoms due to the heavy mass of Cr. Further, the number of Al atoms nearest Nd is larger than the number of Cr atoms, which also means that the contribution of Al to the spectra is larger than that of Cr. Secondly, the distances between Cr and its nearest four Al atoms at the 8*i* site and four Al at the 8*j* site are 2.81 and 2.68 Å, respectively. Since the curve $\Phi_{Cr-Al}(r)$ is deep and narrow, Cr also reacts strongly with these Al atoms, which means that the Al atoms contribute to the higher frequency modes due to the light mass of Al. Finally, as shown in Fig. 1a, the very strong interaction between Cr and Cr at their nearest distance (2.69 Å) also cause Cr to vibrate at high frequencies. The different interactions at various distances such as d_{2a-8i} (3.20 Å), d_{2a-8j} (3.32 Å), d_{2a-8f} (3.51 Å), d_{8i-8i} (2.78 Å), d_{8i-8j} (2.98 and 2.96 Å), d_{8i-8f} (2.81 Å), d_{8j-8j} (2.77 Å), d_{8j-8f} (2.68 Å) and d_{8f-8f} (2.69 Å) may explain the multifarious peaks of the spectra.

For the $NdCu_4Al_8$, in the range of 0–4.8 THz, the ratio of the modes excited by Nd, Cu and Al atoms is 2:6:3. In 4.8–9.5 THz, the contribution of Nd to the phonon spectra is almost zero, and the ratio of that of Cu and Al is about 2:9. In the range of 9.5–11.4 THz, the modes excited by Al atoms are ~87%. It is noted that the highest frequency of the vibrational modes for $NdCu_4Al_8$ is much lower than that of $NdCr_4Al_8$. The main peaks in both low and high frequency move toward the lower part. This can be expected by comparing the interaction curves of $NdCu_4Al_8$ with $NdCr_4Al_8$ in Fig. 1a. The interactions, resulting in the higher frequency modes, $\Phi_{Nd-Cu}(r)$, $\Phi_{Cu-Al}(r)$ and $\Phi_{Cu-Cu}(r)$ are weaker than $\Phi_{Nd-Cr}(r)$, $\Phi_{Cr-Al}(r)$ and $\Phi_{Cr-Cr}(r)$, respectively, at the nearest neighbors. In addition, the mass of Cu is heavier than that of Cr, which also induces lower frequency modes.

In the NdT_4Al_8 (T=Mn, Fe) compounds, the phonon densities of states are similar with that of $NdCr_4Al_8$ mentioned above. For the SmT_4Al_8 (T=Cr, Cu, Mn, Fe) compounds, the interactions $\Phi_{Sm-Al}(r)$, $\Phi_{Sm-Cr}(r)$, $\Phi_{Sm-Cu}(r)$ and $\Phi_{Sm-Mn}(r)$ are close to $\Phi_{Nd-Al}(r)$, $\Phi_{Nd-Cr}(r)$, $\Phi_{Nd-Cu}(r)$ and $\Phi_{Nd-Mn}(r)$, respectively, at their nearest distances, which entails that the corresponding DOS of SmT_4Al_8 (Fig. 3) are similar with those of NdT_4Al_8. As is expected, the highest frequencies of the former are little higher than those of the latter because the mass of Sm is larger than that of Nd, which confines the motions of Al and the ternary elements and intensifies their vibrations.

Furthermore, the dependences of the Debye temperature on the temperature for NdT_4Al_8 and SmT_4Al_8 (T=Cr, Cu, Fe, Mn) were derived from the calculated phonon densities of states. The values of the Debye temperature near 0 K of these compounds are listed in Table 7. It can be seen that the values of Debye temperature and Einstein temperature are largest for $NdFe_4Al_8$ and $SmFe_4Al_8$ and smallest for $NdCu_4Al_8$ and $SmCu_4Al_8$. Fig. 4 presents the dependences

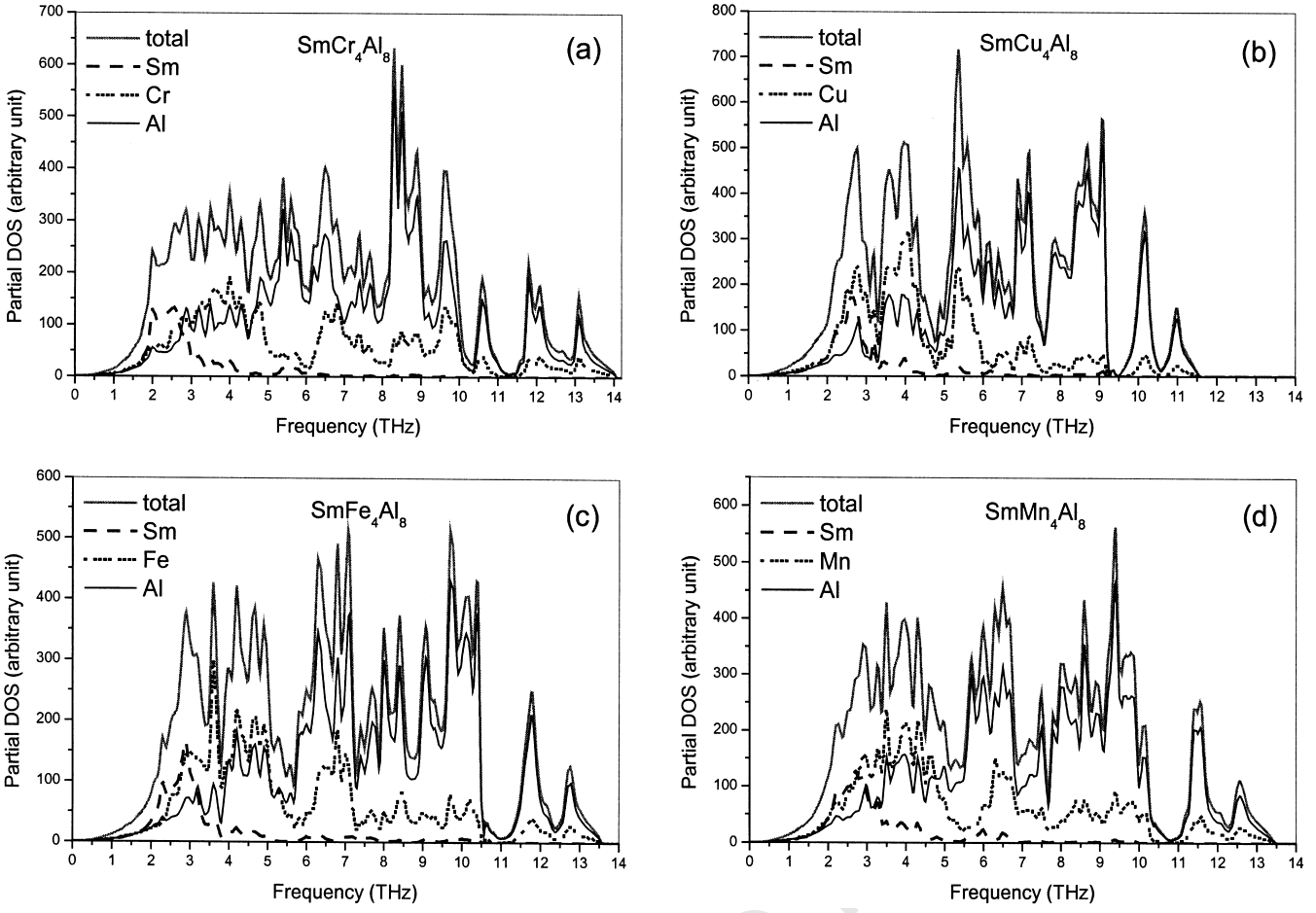

Fig. 3. Phonon densities of states of $SmCr_4Al_8$ (a), $SmCu_4Al_8$ (b), $SmFe_4Al_8$ (c) and $SmMn_4Al_8$ (d).

of the Debye temperature on the temperature NdT_4Al_8. Unfortunately, so far, the above calculations have not been verified by experiments.

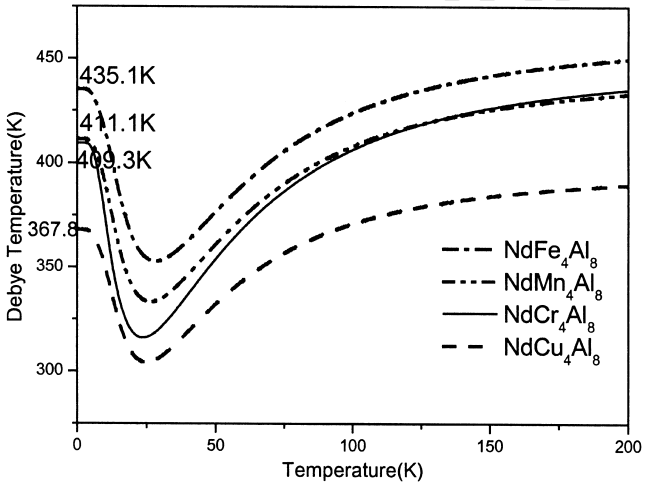

Fig. 4. Debye temperature of NdT_4Al_8 (T=Cr, Cu, Fe, Mn).

6. Conclusion and discussion

In the present study, using the inverted interatomic potentials the calculated lattice constants for NdT_4Al_8 and SmT_4Al_8 (T=Cr, Cu, Fe, Mn) are in good agreement with the experimental data. These potentials are also applied to evaluate the phonon density of states of these materials. Since the present study is perhaps the first lattice dynamical calculations on phonon density of states for these compounds, we could not compare our results with experimental measurements and other work. In the calculations, some of the modes of RAl_{12} (R=Nd, Sm) are soft,

Table 7
Debye temperature Θ_D (K) of $Nd(Al,T)_{12}$ and $Sm(Al,T)_{12}$ (T=Cr, Cu, Mn, Fe)

Materials	Θ_D (K)	Materials	Θ_D (K)
$NdCr_4Al_8$	409.3	$SmCr_4Al_8$	402.9
$NdCu_4Al_8$	367.8	$SmCu_4Al_8$	364.4
$NdMn_4Al_8$	411.1	$SmMn_4Al_8$	407.0
$NdFe_4Al_8$	435.1	$SmFe_4Al_8$	429.1

which agrees with the metastable structure of binary RAl_{12} in the experiments. For the ternary NdT_4Al_8 and SmT_4Al_8 compounds (T=Cr, Cu, Fe and Mn), soft modes do not appear. The ratio of the modes contributed by R, T and Al atoms is 1:4:8 in the total frequency range. However, this ratio will change in the different frequency ranges. The intermediate and high frequency sides of the phonon spectra essentially only involve the vibrations of Al and T atoms. R atoms only vibrate at lower frequency because of their large atomic mass. The qualitative analysis provides a deeper knowledge of the cohesive properties associated with the different crystallographic sites. In summary, in spite of the simplified calculation model employed by us, the inverted potentials method is an effective starting point in the study of rare earth intermetallic compounds with complex structures. Improvement can be achieved by including more factors such as the entropy and temperature and so on.

Acknowledgements

This work is supported in part by the National Nature Science Foundation of China, no. 59971006 and in part by the National Advanced Materials Committee of China and Special Funds for Major State Basic Research of China, no. G2000067101 and no. G2000067106.

References

[1] O. Moze, R.M. Ibberson, K.H.J. Buschow, J. Phys. Condens. Matter 2 (1990) 1677.
[2] P. Schobinger-Papamantellos, K.H.J. Buschow, C. Ritter, J. Magn. Magn. Mater. 186 (1998) 21.
[3] J.A. Paixão, M. Ramos Silva, S.A. Sørensen, B. Lebach, G.H. Lander, P.J. Brown, S. Langridge, E. Talik, A.P. Gonçalves, Phys. Rev. B 61 (2000) 6176.
[4] B.Y. Kotur, A.M. Palasyuk, E. Bauer, H. Michor, G. Hilscher, J. Phys. Condens. Matter 13 (2001) 9421.
[5] W. Suski, T. Cichorek, K. Wochowski, D. Badurski, B.Yu. Kotur, O.J. Bodak, Physica B 230–232 (1997) 324.
[6] I.M. Torrens, Interatomic Potentials, Academic Press, New York, 1972.
[7] R.A. Johnson, Phys. Rev. B 39 (1989) 12544.
[8] S.P. Chen, M. Yan, J.D. Gale, R.W. Grimes, R. Devanathan, K.E. Sickafus, N. Yu, M. Nastasi, Phil. Mag. Lett. 73 (1996) 51.
[9] F. Ercolessi, M. Parrinello, E. Tosatti, Phil. Mag. A 58 (1988) 213.
[10] M.W. Finnis, J.E. Sinclair, Phil. Mag. A 50 (1984) 45.
[11] G.J. Ackland, Phil. Mag. A 66 (1992) 917.
[12] M.S. Daw, M.I. Baskes, Phys. Rev. B 29 (1984) 6443.
[13] R.A. Johnson, Phys. Rev. B 41 (1990) 9717.
[14] D.J. Oh, R.A. Johnson, J. Mater. Res. 3 (1988) 471.
[15] K. Hachiya, Y. Ito, J. Phys. Condens. Matter 11 (1999) 6543.
[16] G.M. Bhuiyan, M.A. Khaleque, J. Non-Cryst. Solids 226 (1998) 175.
[17] W.Y. Hu, H.D. Xu, X.L. Shu, X.J. Yuan, B.X. Gao, B.W. Zhang, J. Phys. D Appl. Phys. 33 (2000) 711.
[18] K. Hachiya, Y. Ito, J. Alloys Comp. 279 (1998) 171.
[19] N.X. Chen, Phys. Rev. Lett. 64 (1990) 1193.
[20] N.X. Chen, Z.D. Chen, Y.C. Wei, Phys. Rev. E 55 (1997) R5.
[21] W.Q. Zhang, Q. Xie, X.J. Ge, N.X. Chen, J. Appl. Phys. 82 (1997) 578.
[22] N.X. Chen, X.J. Ge, W.Q. Zhang, F.W. Zhu, Phys. Rev. B 57 (1998) 14203.
[23] A.E. Carlsson, C.D. Gelatt, H. Ehrenreich, Phil. Mag. A 41 (1980) 241.
[24] X.D. Ni, N.X. Chen, J. Shen, J. Mater. Res. 16 (2001) 344.
[25] Y. Liu, N.X. Chen, Y.M. Kang, Mod. Phys. Lett. B 16 (2002) 187.
[26] S.J. Liu, S.Q. Shi, H. Huang, C.H. Woo, J. Alloys Comp. 330–332 (2002) 64.
[27] N.X. Chen, J. Shen, X.P. Su, J. Phys. Condens. Matter 13 (2001) 2727.
[28] Y.M. Kang, N.X. Chen, J. Shen, J. Phys. Chem. Solid., in press.
[29] N.X. Chen, S.Q. Hao, Y. Wu, J. Shen, J. Magn. Magn. Mater. 233 (2001) 169.
[30] H.J. Monkhorst, J.D. Pack, Phys. Rev. B 13 (1976) 5188.
[31] A.R. Williams, J. Kübler, J.R. Gelatt, Phys. Rev. B 19 (1979) 6094.
[32] W. Suski, in: K.A. GschneidnerJr., L. Eyring (Eds.), Handbook on the Physics and Chemistry of Rare Earth, Vol. 22, Elsevier, Amsterdam, 1996, p. 162, Chapter 149.
[33] I. Felner, I. Nowik, J. Phys. Chem. Solids 39 (1978) 951.
[34] O. Moze, R.M. Ibberson, R. Caciuffo, K.H.J. Buschow, J. Less-Common Metals 166 (1990) 329.
[35] J. Gal, H. Pinto, S. Fredo, H. Shaked, W. Schäfer, G. Will, F.J. Litterst, W. Potzel, L. Asch, G.M. Kalvius, Hyperfine Int. 33 (1987) 173.
[36] I. Felner, I. Nowik, J. Phys. Chem. Solids 40 (1979) 1035.
[37] K.H.J. Buschow, J.H.N. van Vucht, W.W. van den Hoogenhof, J. Less-Common Metals 50 (1976) 145.
[38] M. Kuznietz, A.P. Gonçalves, J.C. Waerenborgh, M. Almeida, C.C. Cardoso, M.M. Cruz, M. Godinho, Phys. Rev. B 60 (1999) 9494.
[39] F.G. Vagizov, W. Suski, K. Wochowski, H. Drulis, J. Alloys Comp. 219 (1995) 271.
[40] Y.M. Kang, N.X. Chen, J. Alloys Comp., in press.